TPM Vol. 32, No. S7, 2025
ISSN: 1972-6325
https://www.tpmap.org/

MODEL PREDICTIVE CONTROL OF PERMANENT MAGNET SYNCHRONOUS ROUND MOTOR FOR HEAVY-DUTY VEHICLES

NURSAID POLATER[1*]
[1] DEPARTMENT OF ELECTRICAL AND ELECTRONICS ENGINEERING, YOZGAT BOZOK UNIVERSITY, YOZGAT, TURKEY, nursaid.polater@yobu.edu.tr

Abstract— This research study investigates the design of model predictive control (MPC) for permanent magnet synchronous round machines (PMSRM), employed for heavy-duty vehicular applications. PMSRMs have remarkable potential owing to their power density and efficiency. The target of this study is to explore the MPC method for a particular PMSRM that has parameters of a typical light railway traction motor. Besides, a benchmarking of the PMSRM and MPC model, dynamic analysis of the motor is presented with simulation results. Based on the aim, the MPC algorithm is modelled and implemented in MATLAB/Simulink software tool then the results are compared with traditional field-oriented control (FOC) at the end of the article. According to simulation results, MPC increases torque smoothness and drastically lowers current ripple, increasing robustness and energy efficiency. By modifying predictive control for high-inertia, rail-specific PMSRMs, this study advances the field and aids in the implementation of low-carbon railway transport projects.

Keywords— electric vehicles, field-oriented control, model predictive control, PMSRM, railway traction.

I. INTRODUCTION

Now more than ever, the electrification of transportation represents an important asset for transport stakeholders to meet the policies of decarbonisation. There are a lot of underlying reasons for making an action plan for decarbonisation and taking measures to do so to improve the transport sector. First, the quarter of greenhouse gas emitter is the transportation industry, and emissions of hazardous gases have remained almost stable since the 1990s. Additionally, according to the EU Department of Transport, the number of electric vehicles is rising gradually, and the governments' plan to fully stop selling cars with internal combustion engines over the next decades to be able to the transportation industry will become carbon-free as a result [1, 2, 3].

Due to the environmental issues described above, the International Railway Association defined two objectives, namely reducing emissions by 2030 and switching to a more sustainable scheme by 2050. The first will be addressed by energy management with technical improvement, whilst the second will be achieved by a modal shift scenario duplicating the share of railway passengers within the transport sector [4]. Therefore, the proposed control scheme with traction motor is designed as a technical improvement for electrified heavy-duty railway applications that operate in the transport sector.

Railway traction systems have been around since the 1800s, and there have been many changes since then. In the early 1800s, diesel traction systems were introduced to cut operating costs; however, they did not meet the reliability and power requirements sufficiently for railway traction [5, 6, 7]. Because it integrates the benefits of both diesel engines and electric machines, diesel-electric traction was therefore thought to be a more effective propulsion method [8]. The dearth of primary energy sources in the latter half of the 20th century then made electric and hybrid traction [6, 9] appealing. Finally fully electrified traction system is used in modern railway applications to reduce carbon emissions. However, this solution requires a high capital cost for infrastructure to build a catenary system or third rail systems for the electrification of traction module. But then, a catenary-free battery, fuel cell, supercapacitor hybrid traction system is under consideration nowadays for the advanced railway traction system.

Reliability, durability, affordability, and ease of servicing are among the characteristics of traction systems that are specified in [10]. Also, the most widely used electric machines in the transport sector are investigated in [11] and [12]. For these reasons, the efficiency of the traction motor and power density are crucial components for electric vehicles that satisfy those criteria. In light of the given traction requirements, decarbonisation goals and current trends in the transportation sector. PMSRMs are seen optimal sort of traction motor for heavy-duty railway applications, where they increase the efficiency of the traction unit and supply powerful tractive performance. Hence, the merits of motor control are the next step for reliability and robustness aspects of the power conditioning

unit. The maturity and performance of FOC for motor drive applications are undeniable facts. However, there are sophisticated and potent options to deal with multivariable parameter monitoring, system-level limitations and actuator coordination effectively in terms of energy management of resources, which is accomplished by MPC. In recent years, a number of research have investigated MPC in traction systems and PMSMs. It has become increasingly important in up-to-date advancements in motor control for electric drives, especially its real-time handling of system restrictions, tracking of variable references, and management of multi-variable systems [13,14]. For example, Lyu et al. [15] increased transient response and decreased torque ripple by compensating for parameter mismatches and creating a limited control set MPC for interior PMSMs in electric car drivetrains. A computationally effective MPC architecture for interior permanent magnet synchronous motor (IPMSM)s was presented by Hassan et al. [16], allowing for real-time application in power-electronic converters. When finite control set model predictive control (FCS-MPC) was used in a salient pole PMSM for electric car use, Murali et al. [17] noted better torque performance and lower harmonic content.

However, the majority of MPC studies that are currently available either concentrate on general-purpose electric machines, hybrid vehicle applications, or IPMSMs. Few works have examined round rotor PMSMs, especially in heavy-duty rail environments where dynamic load fluctuations and high inertia are prevalent. This study closes that gap by modifying MPC control to a PMSRM design and evaluating its performance in a simulated environment configured for typical light railway traction.

The following is how this study is integrated. The dynamic analysis of PMSRM is covered in Section 2, and MPC techniques specifically created for PMSRM drives are covered in Section 3. For the purpose of validation in Section 4, the control architecture is then constructed using the MATLAB/Simulink tool. Section 5 concludes by assessing and contrasting the simulation findings with those of the conventional FOC design.

The unique use of MPC to a PMSRM intended for railway traction applications is what makes this study special. The suggested method allows real-time optimisation of multi-variable control inputs under system restrictions, in contrast to traditional FOC procedures. The following are the contributions made by this paper: A discrete-time predictive control model tailored for PMSRMs was developed and then integrated into a comprehensive simulation framework that replicated actual railway motor conditions; and a comparative performance analysis revealed better steady-state and transient response under MPC. This is a pertinent and timely contribution because, as far as the author is aware, few research have used MPC to round rotor PMSMs for railway transportation.

II. DYNAMIC ANALYSIS OF PMSRM

The mathematical model of the three-phase PMSRM has prime importance in applying control architecture. Therefore, the derivation of motor equations is the initial point to develop MPC for the proposed motor. As for the technical analysis, torque production is based on the development of the excitation field by the magnets, which is the only difference from a wound rotor synchronous motor, and the magnetic field rotates synchronously in the air gap. When excitation and magnetic field rotate at the same speed, electromagnetic or alignment torque is produced by their interactions. For instance, [18] clearly explained the mathematical model of the PMSRM machine, and in [19], the three-phase PMSRM model is manipulated into multiple three-phase counterparts.

In order to get good motor performance within variable working conditions, analysis starts with the extraction of voltage, current, flux, torque, and power equations. Mathematical equations consist of d-q rotating reference frames. The voltage and flux equations are

$u_s = R_s i_s + \frac{d\psi_s}{d_t}$	(1)
$\psi_s = L_s i_s + \psi_{pm}$	(2)

Where u_s, i_s ψ_s , L_s, R_s , ψ_{pm} are voltage, current, flux linkage, self-inductance, the resistance of the stator, and the value of magnetic flux generated by the permanent magnet, respectively. The subscript s refers to the stator. These voltage and flux equations are given for one phase and can be written for three phases in matrix form as given below.

$u_s = [u_A \quad u_B \quad u_C]^T$	(3)
$i_s = [i_A \quad i_B \quad i_C]^T$	(4)
$\psi_s = [\psi_A \quad \psi_B \quad \psi_C]^T$	(5)
$R_s = R_s I_{3x3}$	(6)

In order to simplify the equations, Clarke-Park transformation matrices are applied to the variables. Thus, three-phase systems can be converted into dq rotational reference frames as follows.

$$\begin{bmatrix} u_d \\ u_q \end{bmatrix} = \begin{bmatrix} R_s & 0 \\ 0 & R_s \end{bmatrix} \begin{bmatrix} i_d \\ i_q \end{bmatrix} + \frac{d}{dt} \begin{bmatrix} \psi_d \\ \psi_q \end{bmatrix} + \omega \begin{bmatrix} -\sin\theta \\ \cos\theta \end{bmatrix} \quad (7)$$

$$\begin{bmatrix} \psi_d \\ \psi_q \end{bmatrix} = \begin{bmatrix} L_d & 0 \\ 0 & L_q \end{bmatrix} \begin{bmatrix} i_d \\ i_q \end{bmatrix} + \begin{bmatrix} \psi_{pm} \\ 0 \end{bmatrix} \quad (8)$$

In the given matrix equations ψ, L, i, ω are the flux linkage, the self-inductance, the current, electrical angular speed of a machine, respectively, and the subscript d refers to the d-axis component, q to the q-axis component of winding sets.

Due to the utilisation of three-phase PMSRM, $L_d = L_q$ assumption could be made to derive the flux linkage and voltage equations of the stator.

$$\psi_d = L_d i_d + \psi_{pm}$$
$$\psi_q = L_q i_q \quad (9)$$

The stator equations can be expressed as follows.

$$u_d = R_s i_d + \frac{d\psi_d}{dt} - \omega\psi_q = R_s i_d + L_d \frac{di_d}{dt} - \omega L_q i_q \quad (10)$$

$$u_q = R_s i_q + \frac{d\psi_q}{dt} + \omega\psi_d = R_s i_q + L_q \frac{di_q}{d_t} + \omega L_d i_d + \omega\psi_m \quad (11)$$

Now, magnetic cross-coupling equations have been obtained. A rotating reference frame (RF) is used with FOC and MPC in simulation and calculations. Therefore, general equations are needed and are given below [18].

The instantaneous input power of the PMSRM is

$$P_{in} = \frac{3}{2}(v_d i_d + v_q i_q) \quad (12)$$

Electromagnetic power is expressed as

$$P_{el} = P_{in} - P_{Cu} \quad (13)$$

$$P_{el} = \frac{3}{2}\omega(\psi_d i_q - \psi_q i_d) \quad (14)$$

The motor electromagnetic torque is given by

$$T_e = \frac{P_{el}}{\omega_m} \quad (15)$$

$$T_e = \frac{3}{2}p(\psi_d i_q - \psi_q i_d)$$
$$= \frac{3}{2}p[\psi_{pm}(i_q) + (L_d - L_q)(i_d i_q)] \quad (16)$$

Where ω_m is the mechanical angular speed of a machine, which corresponds to the electrical angular speed, ω and the number of motor pole pairs, P, by

$$\omega_m = \omega/P \quad (17)$$

III. Model Predictive Control for PMSRM

MPC is getting popular for motor drives and converter applications due to enabling multivariable parameter tracking, evaluation of system constraints, and coordination of actuators efficiently in terms of management of energy resources.

The system is controlled with a prediction model and a reference state at every single sampling time, where there exists an optimal solution for the control horizon within a certain time frame [20]. The aforementioned trackable of multivariable simultaneously, considerability of the system's input/output, monitoring multiple target references, and efficiency of actuator management and coordination of supply sources are seen as advantageous for MPC.

A cost function, a converter predictive model, and a load model are the three primary components of an MPC. The motor itself serves as the load for the PMSRM's control. Figure 1 displays the block diagram of the whole control arrangement. A model of prediction comprising parts 2 and 3 yields a predictive current. Part 1's inputs are the current reference and the predicted current. If a static power converter can be regulated by a finite set of switching states, such states are predicted by a Model Predictive Controller (MPC) based on criteria that calculate prediction elements. This parameter is referred to as the cost function. This function predicts future variables for

the system or the inverter's switching pattern. The state that minimises the cost function is generally the standard of reference.

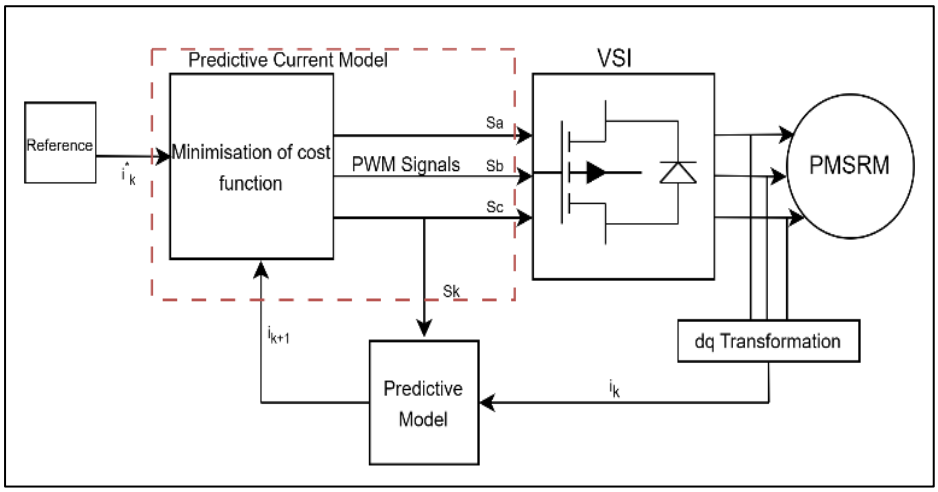

Fig. 1 Block Diagram of MPC for PMSRM

The discretised dynamic functions of the predictive model from Equations (10) and (11) can be expressed as

$$u_{d(k)} = R_s i_{d(k)} + \frac{L_d}{T_s}[i_{d(k+1)} - i_{d(k)}] - \omega L_q i_{q(k)} \quad (18)$$

$$u_{q(k)} = R_s i_{q(k)} + \frac{L_q}{T_s}[i_{q(k+1)} - i_{q(k)}] + \omega L_d i_{d(k)} + \omega \psi_m \quad (19)$$

The discrete currents derived from 18-19 according to the dynamic functions are

$$i_{d(k+1)} = i_{d(k)} + \frac{T_s}{L_d}[v_{d(k)} - R_s i_{d(k)} + \omega_r L_q i_{q(k)}] \quad (20)$$

$$i_{q(k+1)} = i_{q(k)} + \frac{T_s}{L_q}[v_{q(k)} - R_s i_{q(k)} - \omega L_d i_{d(k)} - \omega \psi_m] \quad (21)$$

IV. SIMULATION RESULTS

This section presents the PMSRM simulation findings and the Simulink model. For modelling, certain specific data needs to be identified, which includes motor parameters and specs of the railway application. For this purpose, the machine's characteristics are displayed in Table I below, where rated values of the PMSR are given in the nameplate like leakage inductances, rated current, rated voltage of the motor and typical light railway datasets such as load of inertia, maximum speed, typical gear ratio and number of passengers etc.

Table I.. DATASHEET OF PMSRM

Rated Speed (RPM)	1500
Train Rated Speed (km/h)	40
Rated Torque (Nm)	740
Rated Power (kW)	110
Switching Frequency (kHz)	5
Rated Voltage	359
Rated Current	191
No-load Voltage at 1000 RPM	229
Phase Resistance (Ω)	0.0088
Ld and Lq Inductances (mH)	1.104
Train Mass (Tone)	150
Gear ratio (G)	6
Wheel Diameter (m)	0.5
Motor Moment and Load of Inertia (kg. m^2)	50.85

TPM Vol. 32, No. S7, 2025
ISSN: 1972-6325
https://www.tpmap.org/

Open Access

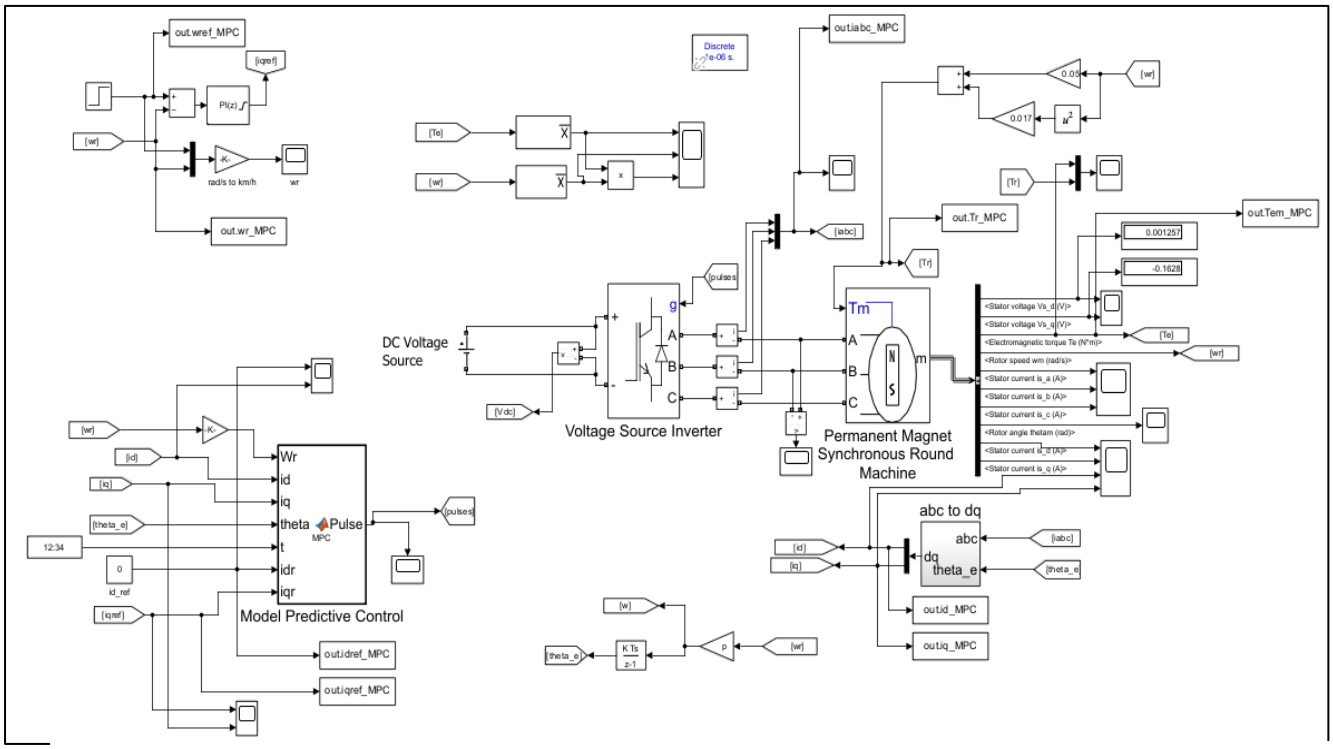

Fig. 2 The complete Simulink Architecture

The complete Simulink architecture is given in Figure 2, where is constructed DC source, a three-phase IGBT voltage source inverter (VSI), a motor, abc to dq transformation blocks, a MATLAB function block where MPC is implemented, and complementary blocks for both references and measurements.

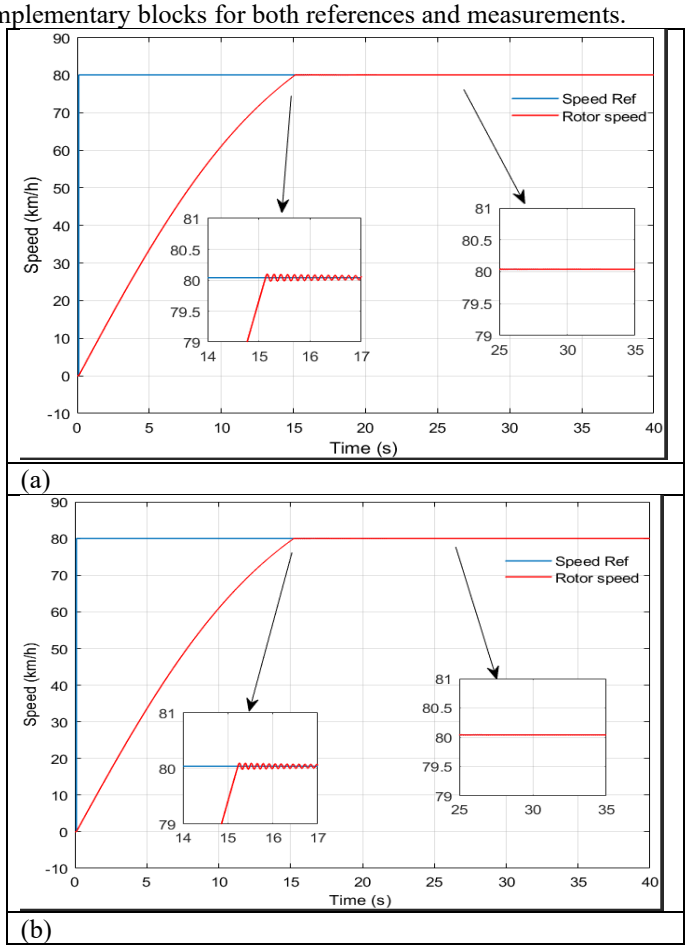

Fig. 3 Comparison of Speed Waveforms of PMSRM for a) FOC and b) MPC methods

The PMSRM has quite a similar acceleration rate while controlled by both MPC and FOC, and Figure 3 illustrates the acceleration rate of PMSRM. There exists a smooth transition from transient response to steady state condition, and the error is pretty small for both techniques.

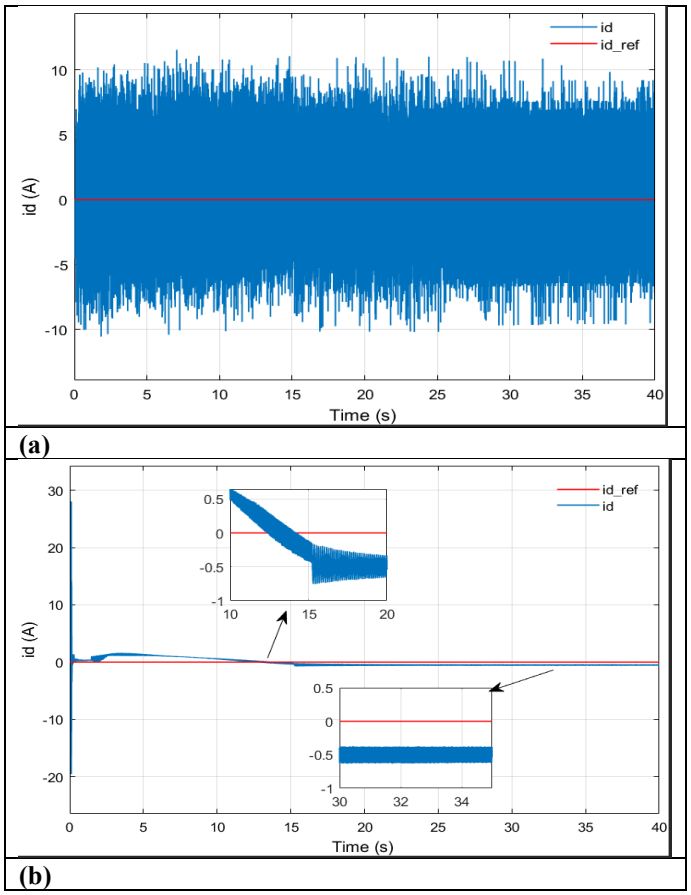

Fig. 4 Comparison of id Currents of PMSRM for a) FOC and b) MPC methods

id currents are also set to zero because to round rotor PMSM is used in this research. Then implementation of the id=0 control, currents follow the references as given in Figure 4. The current waveform has lots of oscillations between +10 and -10A for FOC controlled PMSRM, while these fluctuations are reduced between +2 and -2A for MPC controlled machine in Figure 4-(a) and (b) respectively.

It is important to note that there exists a quite big spike at the initial operation of the MPC-controlled machine, but this would not last a long period and is compensated at the beginning of operation. Additionally, whenever speed reaches to rated value, the measured id current does not fluctuate during the steady state condition, and there exists nearly 0.5 a error as given in Figure 4-(b).

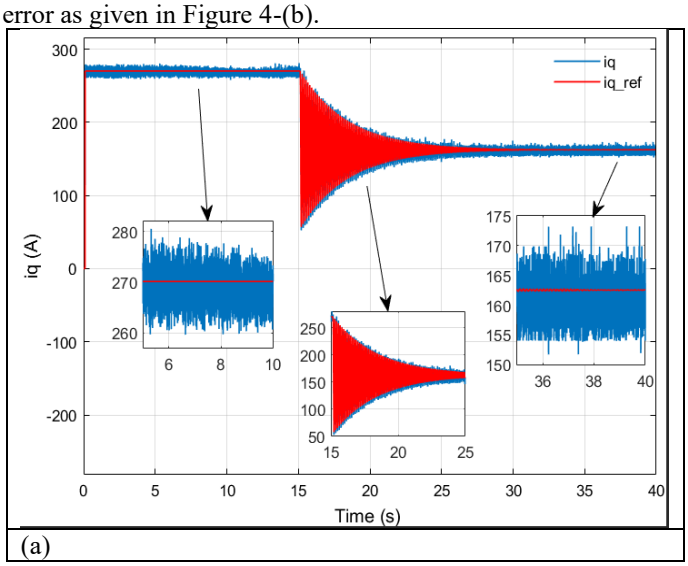

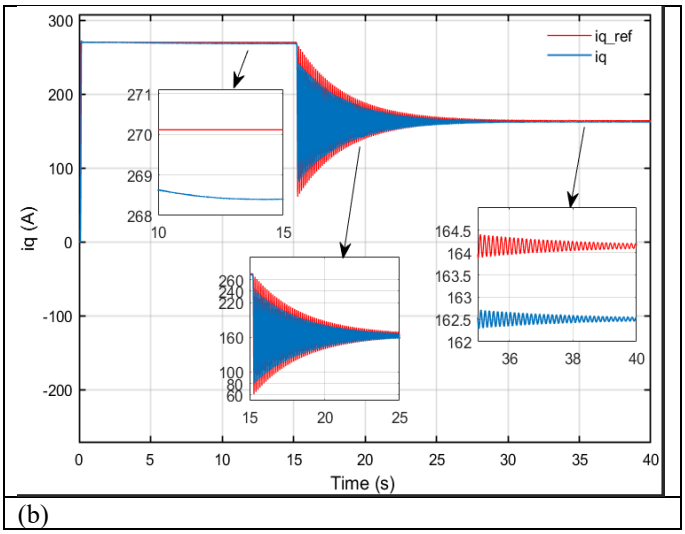

Fig. 5 Comparison of iq Currents of PMSRM for a) FOC and b) MPC methods

The iq currents' graphs are given in Figure 5, where current oscillations around 260-280A can be observed during the acceleration period from 0 to 15 seconds for Figure 5-(a), while these fluctuations are decreased massively by using MPC, shown in Figure 5-(b).

On the other hand, there exist oscillations both in MPC and FOC during the transition period between 15 and 25 seconds because of the transient response of the controller. However, these oscillations are also relatively less for MPC since it starts between 80 and 240A, whereas this range is 50 to 260A for the FOC method.

After the given fluctuation period, the MPC shows better performance compared to FOC during the steady state condition from 30 to 40 seconds. The current iq varies between 155 and 170A in Figure 5-(a), while this value is around 162.5A for MPC given in Figure 5-(b), even though the existence of steady state error for MPC.

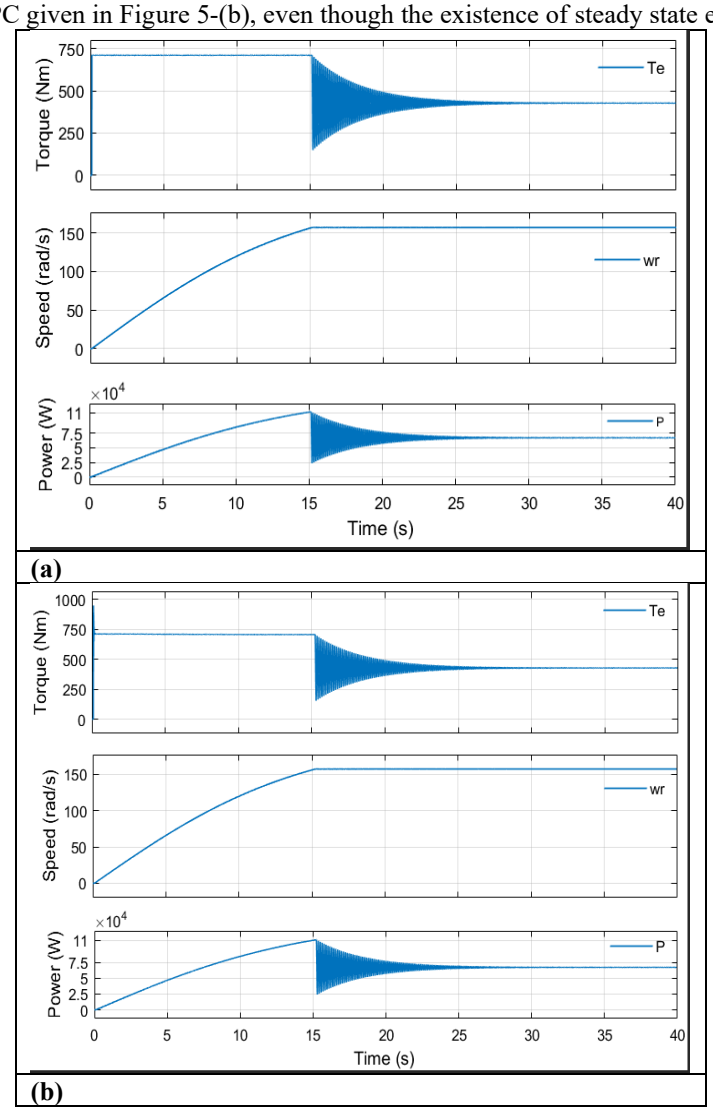

Fig. 6 Comparison of Torque, Angular Motor Speed and Output Power of PMSRM for a) FOC and b) MPC methods

Finally, Figure 6 demonstrate the torque, angular speed of the PMSRM, and output power of the traction system where nominal torque is 740Nm, rated output power is 110kW, and rated speed of motor is 157 rad/s given in the Table II. İt is obvious that train is accelerating first 15 second and during this transient period speed and power are increasing until they reach to the rated value while torque is constant to provide maximum tractive effort for the traction system. Then, the aforementioned parameters are staying stable during the steady state period as they should be.

A. Simulation Setup

A discrete-time modelling architecture in MATLAB/Simulink was used to carry out the suggested control technique. With a time step of 10 µs and a fixed-step solver, the simulation time was set at 40 seconds. A MATLAB Function block that takes in motor state data and outputs inverter switching signals determined by cost function minimisation was used to write the MPC algorithm.

As is common in finite control set MPC, the control horizon was set at 1 step, while the prediction horizon was set at 1 step ahead, or 10 µs. The definition of the cost function was:

$$g(i_{dq}{}^{*}, i_{dq}) = (i_d^* - i_d)^2 + (i_q^* - i_q)^2 \quad (22)$$

where idq is the motor model's projected value and idq* is the reference current. Beyond converter limits, no strict restrictions were imposed.

In accordance with the hardware requirements listed in Table I, the model makes use of a three-phase IGBT-based Voltage Source Inverter (VSI) with a switching frequency of 5 kHz. The dq-transformed voltage equations obtained in Section 2 are used in the PMSRM block. Step commands and filtered ramps were used to create reference currents and speeds.

The FOC implementation employed pole placement method for tuning the PI controllers to reduce overshoot and settling time in order to guarantee fairness.

V. CONCLUSIONS

The employed model is a round rotor PMSM and has DC power sources to drive a 110 kW motor via a 750V DC source. This type of traction configuration is useful for the electrified or modular catenary-free railways like battery, fuel cell and supercapacitor, etc. and key parameter indicators has been compared in Table II. It can be clearly seen from the simulation results that the control architecture has an important effect on the current ripple and the ripple relevant to the current, such as power and torque. Those fluctuations are linked with the power losses and have crucial importance for the traction system efficiency.

As it is proven in the simulation result that MPC performs better for the q-axis current and d-axis current profiles in terms of oscillation for a given reference frame compared to FOC. In addition, it is obvious that MPC performance fulfils much better the robustness and reliability requirements for a given heavy-duty application by having an acceptable current ripple range compared to FOC.

The system is more effective for traction situations in the real world because of the enhanced current tracking and less ripple, which immediately result in fewer energy losses. According to these findings, MPC can greatly improve the robustness and performance of electrified railway systems, especially those that use fuel cells or batteries as catenary-free energy sources.

This research paper has summarised the modelling and analysis of controller methods for PMSRM employed in a typical light railway application. At the beginning, general policies and general consensus are discussed. Then, the requirements of the traction system of a light railway are addressed. Followed by dynamic modelling of a PMSRM and an MPC is derived for a technical analysis and Simulink implementation. Finally, simulation results are discussed, and dq currents' profiles are assessed in terms of efficiency and robustness.

Future steps include extending the predictive controller to manage energy storage and mitigate malfunction circumstances, as well as conducting experimental validation on a physical test bench. Additionally, performance under changing load and temperature conditions may be enhanced by including online parameter modification.

Table II.. Summarised Comparison Chart for the Recent Studies and Current Research

Study	Motor Type	Application	Control Method	Key Results	Gap Addressed by This Work
Fang et al. (2021) [21]	Traction PMSM	Railway traction motor	FCS-MPC with voltage vector clamping	Enabled six-step over-modulation; validated experimentally	Did not consider round-rotor PMSRM or high-inertia simulation

Peng & Yao (2023) [22]	Various PMSM types	General PMSM drive control	Review of MPC approaches	Summarised robust control techniques and real-time trends	Survey, no traction-specific modeling
Wang et al. (2024) [23]	PMSM	Industrial drive applications	MPC with low switching frequency	Showed practical MPC feasibility under switching limits	Not tested in railway environments
Hassan et al. (2022) [16]	Interior PMSM	Industrial drives	Computationally efficient Model Predictive Current Control (MPCC)	Real-time MPC feasible for traction-like contexts	Not applied to round rotor PMSRM
Murali et al. (2021) [17]	Salient-pole PMSM	EV drives	Finite-Control-Set Model Predictive Current Control (FCS-MPC) speed & torque control	Better transient and torque tracking vs FOC	Small-scale EV motor, not railway traction
Lyu et al. (2021) [15]	IPMSM	General drives	FCS-MPC with parameter mismatch compensation regime	Reduced current ripple and tracking error	No round-rotor PMSM, not in rail inertia
Wen et al. (2024) [14]	PMSM	Torque disturbance handling	MPC + ESO	Fast response to torque disturbances	Not targeted at high-inertia railway application
This Work	Round Rotor PMSM	Catenary-Free Railway	Current-based Discrete MPC	Reduced current ripple, improved torque stability under heavy loads	Applies MPC to high-inertia rail setting with heavy-duty PMSRM model

REFERENCES

[1] Department for Energy Security & Net Zero, , "2023 UK greenhouse gas emissions, provisional figures," National Statistic, 2024.
[2] Department for Transport, "Transport and environment statistics: 2023 (2021 data)," 19 10 2023. [Online]. Available: https://www.gov.uk/government/statistics/transport-and-environment-statistics-2023/transport-and-environment-statistics-2023#:~:text=Transport%20produced%2026%25%20of%20the,road%20vehicles%20(100%20MtCO2e%20).. [Accessed 27 05 2025].
[3] European Commission: Directorate-General for Climate Action, "Going climate-neutral by 2050,Going climate-neutral by 2050 – A strategic long-term vision for a prosperous, modern, competitive and climate-neutral EU economy,Publications Office," 2019. [Online]. Available: https://data.europa.eu/doi/10.2834/02074. [Accessed 27 05 2025].
[4] A. Hoen, A. van Grinsven, B. Kampman, J. Faber, H. van Essen, "Research for TRAN Committee – Decarbonisation of EU transport, European Parliament, Policy Department for Structural and Cohesion Policies," Policy Department, Brussels, 2017.
[5] M. Brenna, F. Foiadelli, D. Zaninelli, Electrical Railway Transportation Systems, NewJersey: IEEE Press Wiley, 2018.
[6] S. Hillmansen, F. Schmid, T. Schmid, "The rise of the permanent-magnet traction motor," Railway Gazette International, pp. 30-34, February 2011.
[7] A. Tessarolo and C. Bassi, "Stator Harmonic Currents in VSI-Fed Synchronous Motors With Multiple Three-Phase Armature Windings," IEEE Transactions on Energy Conversion, vol. 25, no. 4, pp. 974 - 982, 2010.
[8] J. Karttunen, S. Kallio, J. Honkanen, P. Peltoniemi, P. Silventoinen, "Stability and performance of current harmonic controllers for multiphase PMSMs," Control Engineering Practice, vol. 65, p. 59–69, 2017.
[9] S.-H. Kim, Electric Motor Control, Oxford: Elsevier Inc., 2017.
[10] S. Hillmansen, Railway Systems Engineering & Integration Comes of Age, 21st Anniversary Celebration, Birmingham: University of Birmingham, 2015.

[11] C. C. Chan, C. Liu, K. T. Chau, “Overview of permanent-magnet brushless drives for electric and hybrid electric vehicles,” IEEE Trans. Ind. Electron., vol. 55, no. 6, p. 2246–2257, Jun. 2008.
[12] Ş. Kuşdoğan, “Elektrikli otomobillerde enerji depolama sistemlerindeki gelişmeler,” Mühendis ve Makine, vol. 50, no. 596, pp. 2-11, 2009.
[13] T. Li, X. D. Sun, G. Lei, Z. B. Yang, Y. G. Guo, and J. G. Zhu, “Finite-Control-Set Model Predictive Control of Permanent Magnet Synchronous Motor Drive Systems—An Overview,” IEEE/CAA J. Autom. Sinica, vol. 9, no. 12, pp. 2087–2105, Dec. 2022, doi: 10.1109/JAS.2022.105851
[14] D. Wen, X. Wang, Z. Lin, and H. Zhao, “Model Predictive Control With ESO and an Improved Speed Loop Strategy for PMSM Under Load Torque Disturbance,” Progress in Electromagnetics Research Letters, vol. 113, pp. 63–71, 2024, doi: 10.2528/PIERL23122906
[15] Z. Lyu, X. Wu, J. Gao, and G. Tan, “An Improved Finite-Control-Set Model Predictive Current Control for IPMSM under Model Parameter Mismatches,” Energies, vol. 14, no. 19, art. no. 6342, pp. 1–18, Sep. 2021, doi: 10.3390/en14196342
[16] M. Hassan, Y. Khurshid, K. N. Elgazzar, A. F. Zobaa, and A. Hussein, “Computational Efficient Model Predictive Current Control for Interior PMSM,” IET Electric Power Applications, vol. 16, no. 8, pp. 945–959, Aug. 2022, doi: 10.1049/pel2.12294
[17] A. Murali, R. Nadarajah, J. Premkumar, and R. Rajesh, “Assessing Finite Control Set Model Predictive Speed and Torque Controller Performance of a Salient Pole PMSM in EV Application,” Vehicles, vol. 12, no. 1, art. no. 41, Mar. 2021, doi: 10.3390/vehicles4010041
[18] S. Vaez-Zadeh, Control of permanent magnet synchronous motors, Oxford: Oxford University Press, 2018.
[19] E. Levi , M. Bogdan, J. Wilamowski , D. Irwin, “Multiphase AC Machines,” in The Industrial Electronics Handbook Power Electronics and Motor Drives, London, CRC Press, 2011.
[20] M. Tang, S. Zhuang, “On Speed Control of a Permanent Magnet Synchronous Motor with Current Predictive Compensation. ” Energies. 2019; 12(1):65. https://doi.org/10.3390/en12010065
[21] X. Fang, S. Lin, X. Wang, Z. Yang, F. Lin, and Z. Tian, “Model predictive current control of traction permanent magnet synchronous motors in six-step operation for railway application,” IEEE Trans. Ind. Electron., vol. 69, no. 9, 2021, doi: 10.1109/TIE.2021.3114695
[22] J.-Y. Peng and M. Yao, “Overview of Predictive Control Technology for Permanent Magnet Synchronous Motor Systems,” Appl. Sci., vol. 13, no. 10, art. 6255, May 2023. doi: 10.3390/app13106255
[23] S. Wang, Y. Zhang, D. Wu, J. Zhao, and Y. Hu, “Model predictive current control with lower switching frequency for permanent magnet synchronous motor drives,” IET Electr. Power Appl., 2024 (early access)